Physics Letters A 458 (2023) 128573

Contents lists available at ScienceDirect

Physics Letters A

journal homepage: www.elsevier.com/locate/pla

Partial-rogue waves that come from nowhere but leave with a trace in the Sasa-Satsuma equation

Bo Yang [a], Jianke Yang [b,*]

[a] School of Mathematics and Statistics, Ningbo University, Ningbo 315211, China
[b] Department of Mathematics and Statistics, University of Vermont, Burlington, VT 05405, USA

ARTICLE INFO

Article history:
Received 6 October 2022
Received in revised form 30 November 2022
Accepted 1 December 2022
Available online 6 December 2022
Communicated by B. Malomed

Keywords:
Rogue waves
Sasa-Satsuma equation
Generalized Okamoto polynomials

ABSTRACT

Partial-rogue waves, i.e., waves that "come from nowhere but leave with a trace", are analytically predicted and numerically confirmed in the Sasa-Satsuma equation. We show that, among a class of rational solutions in this equation that can be expressed through determinants of 3-reduced Schur polynomials, partial-rogue waves would arise if these rational solutions are of certain orders, where the associated generalized Okamoto polynomials have real but not imaginary roots, or imaginary but not real roots. We further show that, at large negative time, these partial-rogue waves approach the constant-amplitude background, but at large positive time, they split into several fundamental rational solitons, whose numbers are determined by the number of real or imaginary roots in the underlying generalized Okamoto polynomial. Our asymptotic predictions are compared to true solutions, and excellent agreement is observed.

1. Introduction

Rogue waves have been a subject of intensive theoretical and experimental studies in mathematical and physical communities in the past decade. Hundreds of papers and several books have been published on it, and more are still coming. Rogue waves are often defined as "waves that come from nowhere and leave without a trace" [1]. For example, they can be localized wave excitations that arise from the constant-amplitude background, reach higher amplitude, and then retreat back to the same background, as time progresses. Almost all rogue waves that have been theoretically derived or experimentally observed belong to this category (see [2–6], among many others).

However, there exists another type of waves that "come from nowhere but leave with a trace". Specifically, these waves also arise from the constant-amplitude background (thus "come from nowhere"), stay localized, and reach higher amplitude. Afterwards, instead of retreating back to the same constant background with no trace, they evolve into localized waves on the constant background that persist at large time, thus leaving a trace. The first report of such peculiar waves seems to be in [7] for the Davey-Stewartson-II equation, where a two-dimensional localized wave arose from the constant background and then split into two localized lumps at large time (see Fig. 4 of that paper). Later, a similar but one-dimensional solution was reported in [8] for the Sasa-Satsuma equation. These peculiar waves resemble rogue waves in the first half of evolution, but contrast them in the second half of evolution. Due to these peculiar behaviors, let us call them partial-rogue waves. Note that although two examples of partial-rogue waves can be seen in [7,8], there was no explanation for their appearance, as if they were pure accidents. It was also unclear whether additional types of partial-rogue waves could be found in those two systems.

In this paper, we predict partial-rogue waves in the Sasa-Satsuma equation through large-time asymptotic analysis on its rational solutions. We show that, among a class of rational solutions in this equation that can be expressed through determinants of 3-reduced Schur polynomials, partial-rogue waves arise if and only if these rational solutions are of certain orders, where the associated generalized Okamoto polynomials have real but not imaginary roots, or imaginary but not real roots. We further show that, at large negative time, these partial-rogue waves approach the constant-amplitude background, but at large positive time, they split into several fundamental rational solitons, whose numbers are determined by the number of real or imaginary roots in the underlying generalized Okamoto polynomial. Our asymptotic pre-

* Corresponding author.
E-mail address: jxyang@uvm.edu (J. Yang).

https://doi.org/10.1016/j.physleta.2022.128573
0375-9601/

dictions are compared to true solutions, and excellent agreement is observed.

2. Preliminaries

The Sasa-Satsuma equation was proposed as a higher-order nonlinear Schrödinger equation for optical pulses that includes some additional physical effects such as third-order dispersion and self-steepening [9,10]. Through a variable transformation, this equation can be written as

$$u_t = u_{xxx} + 6|u|^2 u_x + 3u(|u|^2)_x. \tag{2.1}$$

Sasa and Satsuma [9] showed that this equation is integrable.

2.1. A class of rational solutions

Soliton solutions on the zero background in this equation were derived by Sasa and Satsuma in their original paper [9]. Later, rational solutions on a nonzero background, including rogue waves, were also derived [8,11–19]. The solutions that will be the starting point of this paper are a certain class of rational solutions, whose τ functions are determinants of 3-reduced Schur polynomials, i.e., determinants of Schur polynomials with index jumps of three. These solutions are different from Sasa-Satsuma rogue waves derived by the bilinear method in [16,17], which were determinants of 2-reduced Schur polynomials. In the language of Darboux transformation, our solutions of 3-reduced Schur polynomials correspond to a scattering matrix admitting a triple eigenvalue. Such solutions have been studied in [8,14] by Darboux transformation. However, their solutions are not general nor explicit for our purpose. For this reason, we will first present general and explicit expressions for this class of rational solutions through Schur polynomials. Derivation of these solutions by the bilinear method will be provided in the appendix.

Before presenting these solutions, we need to specify the nonzero background. Through variable scalings, we can normalize the background amplitude to be unity. Then, this background can be written as

$$u_{bg}(x,t) = e^{\mathrm{i}[\alpha(x+6t)-\alpha^3 t]}, \tag{2.2}$$

where α is a free wavenumber parameter, which cannot be removed since the Sasa-Satsuma equation (2.1) is not Galilean-invariant. But α can be restricted to be positive, since the Sasa-Satsuma equation is invariant under the axes reflection of $(x,t)\to(-x,-t)$, and negative-α solution can be related to positive-α solution through this axes reflection.

To present these explicit rational solutions, we also need to introduce elementary Schur polynomials. These polynomials $S_j(\boldsymbol{x})$ with $\boldsymbol{x}=(x_1,x_2,\ldots)$ are defined by the generating function

$$\sum_{j=0}^{\infty} S_j(\boldsymbol{x})\epsilon^j = \exp\left(\sum_{j=1}^{\infty} x_j \epsilon^j\right). \tag{2.3}$$

In addition, we define $S_j(\boldsymbol{x})=0$ when $j<0$.

Our expressions for general rational solutions whose τ functions are determinants of 3-reduced Schur polynomials are given by the following theorem.

Theorem 1. *When $\alpha=1/2$, the Sasa-Satsuma equation (2.1) admits bounded (N_1,N_2)-th order rational solutions*

$$u_{N_1,N_2}(x,t) = \frac{g_{N_1,N_2}}{f_{N_1,N_2}} e^{\mathrm{i}[\alpha(x+6t)-\alpha^3 t]}, \tag{2.4}$$

where N_1 and N_2 are arbitrary non-negative integers,

$$f_{N_1,N_2} = \sigma_{0,0}, \quad g_{N_1,N_2} = \sigma_{1,0}, \tag{2.5}$$

$$\sigma_{k,l} = \det\begin{pmatrix} \sigma_{k,l}^{[1,1]} & \sigma_{k,l}^{[1,2]} \\ \sigma_{k,l}^{[2,1]} & \sigma_{k,l}^{[2,2]} \end{pmatrix}, \tag{2.6}$$

$$\sigma_{k,l}^{[I,J]} = \left(\phi_{3i-I,3j-J}^{(k,l\,I,J)}\right)_{1\le i\le N_I,\,1\le j\le N_J}, \tag{2.7}$$

matrix elements in $\sigma_{k,l}^{[I,J]}$ are defined by

$$\phi_{i,j}^{(k,l,I,J)} = \sum_{\nu=0}^{\min(i,j)} \left(\frac{p_1^2}{4p_0^2}\right)^{\nu} \times S_{i-\nu}(\boldsymbol{x}_I^+(k,l)+\nu\boldsymbol{s})\, S_{j-\nu}(\boldsymbol{x}_J^-(k,l)+\nu\boldsymbol{s}), \tag{2.8}$$

vectors $\boldsymbol{x}_I^{\pm}(k,l)=(x_{1,I}^{\pm},x_{2,I}^{\pm},\cdots)$ are given by

$$x_{r,I}^{+}(k,l) = p_r(x+6t)+\beta_r t + k\theta_r + l\theta_r^* + a_{r,I}, \tag{2.9}$$

$$x_{r,J}^{-}(k,l) = p_r(x+6t)+\beta_r t - k\theta_r^* - l\theta_r + a_{r,J}, \tag{2.10}$$

β_r and θ_r are coefficients from expansions

$$p^3(\kappa) = \sum_{r=0}^{\infty}\beta_r\kappa^r, \ \ln\left[\frac{p(\kappa)-\mathrm{i}\alpha}{p_0-\mathrm{i}\alpha}\right] = \sum_{r=1}^{\infty}\theta_r\kappa^r, \tag{2.11}$$

the function $p(\kappa)$ with expansion $p(\kappa)=\sum_{r=0}^{\infty}p_r\kappa^r$ and real expansion coefficients p_r is defined by the equation

$$Q_1[p(\kappa)] = \frac{Q_1(p_0)}{3}\left[e^{\kappa}+2e^{-\kappa/2}\cos\left(\frac{\sqrt{3}}{2}\kappa\right)\right], \tag{2.12}$$

with

$$Q_1(p) \equiv \frac{1}{p-\mathrm{i}\alpha}+\frac{1}{p+\mathrm{i}\alpha}+p, \tag{2.13}$$

$p_0=\pm\sqrt{3}/2$, the real vector $\boldsymbol{s}=(s_1,s_2,\cdots)$ is defined by the expansion

$$\ln\left[\left(\frac{2p_0}{p_1\kappa}\right)\left(\frac{p(\kappa)-p_0}{p(\kappa)+p_0}\right)\right] = \sum_{r=1}^{\infty}s_r\kappa^r, \tag{2.14}$$

the asterisk '' represents complex conjugation, and*

$$(a_{1,1},\cdots,a_{3N_1-1,1}),\ (a_{1,2},\cdots,a_{3N_2-2,2}) \tag{2.15}$$

are free real constants.

The proof of this theorem by the bilinear method will be given in the appendix.

Note 1. When we choose $p_0=\sqrt{3}/2$, the first few coefficients of p_r, β_r, θ_r, and s_r are

$$p_1 = \frac{12^{1/6}}{2}, \quad p_2 = \frac{12^{-1/6}}{2}, \quad p_3 = \frac{1}{4\sqrt{3}}, \tag{2.16}$$

$$\beta_1 = \frac{9}{8}12^{1/6}, \quad \beta_2 = \frac{9}{8}\cdot\frac{3^{5/6}}{2^{1/3}}, \quad \beta_3 = \frac{19\sqrt{3}}{16}, \tag{2.17}$$

$$\theta_1 = \frac{12^{1/6}}{\sqrt{3}-\mathrm{i}}, \quad \theta_2 = \frac{-\mathrm{i}}{12^{1/6}\left(\sqrt{3}-\mathrm{i}\right)^2}, \quad \theta_3 = 0, \tag{2.18}$$

$$s_1 = 0, \quad s_2 = 0, \quad s_3 = -\frac{1}{40}. \tag{2.19}$$

If we choose $p_0=-\sqrt{3}/2$, then p_r and β_r would switch sign, θ_r change to θ_r^*, and s_r remain the same.

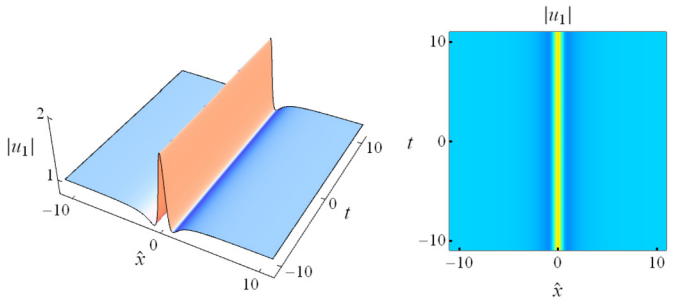

Fig. 1. Graph of the fundamental rational soliton $|u_1(x,t)|$ in Eq. (2.20). Left: 3D plot. Right: density plot. The horizontal axes are $\hat{x} = x + (33/4)t$.

Note 2. If we choose $p_0 = -\sqrt{3}/2$ and keep all internal parameters $(a_{r,1}, a_{r,2})$ unchanged, then the resulting solution $\tilde{u}(x,t)$ would be related to the solution $u(x,t)$ with $p_0 = \sqrt{3}/2$ as $\tilde{u}(x,t) = u^*(-x,-t)$.

Note 3. Internal parameters $a_{3n,1}$ and $a_{3n,2}$ $(n = 1, 2, \cdots)$ do not affect solutions in Theorem 1, for reasons which can be found in [20]. Thus, we will set them as zero in later text.

The simplest solution of this class – the fundamental rational soliton, is obtained when we set $N_1 = 0$ and $N_2 = 1$ in Theorem 1. In this case, the solution has a single real parameter $a_{1,2}$, which can be normalized to zero through a shift of the x axis. The resulting solution, for both $p_0 = \pm\sqrt{3}/2$, is

$$u_1(x,t) = \hat{u}_1(x,t) e^{\mathrm{i}[\frac{1}{2}(x+6t) - \frac{1}{8}t]}, \tag{2.20}$$

where

$$\hat{u}_1(x,t) = \frac{3\hat{x}^2 + 3\mathrm{i}\hat{x} - 2}{3\hat{x}^2 + 1}, \tag{2.21}$$

and

$$\hat{x} \equiv x + \frac{33}{4}t \tag{2.22}$$

is a moving coordinate. The graph of this solution is plotted in Fig. 1. This solution is a rational soliton moving on the constant-amplitude background (2.2) with velocity $-33/4$. Its 3D graph shows a W-shape along the $\hat{x}$ direction and has sometimes been called a W-shaped rational soliton in the literature [8,18]. Its height, i.e., $\max(|u_1|)$, is 2.

2.2. Generalized Okamoto polynomials

We will show in later text that rational solutions in Theorem 1 contain partial-rogue waves but are not all partial-rogue waves. The question of what solutions in Theorem 1 are partial-rogue waves turns out to be closely related to root properties of generalized Okamoto polynomials. So, we will introduce these polynomials and examine their root structures next.

Original Okamoto polynomials arose in Okamoto's study of rational solutions to the Painlevé IV equation [21]. He showed that a class of such rational solutions can be expressed as the logarithmic derivative of certain special polynomials, which are now called Okamoto polynomials. These original polynomials were later generalized, and the generalized Okamoto polynomials provide a more complete set of rational solutions to the Painlevé IV equation [22–25]. In addition, determinant expressions for the original and generalized Okamoto polynomials were discovered [22–25].

Let $p_j(z)$ be Schur polynomials defined by

$$\sum_{j=0}^{\infty} p_j(z)\epsilon^j = \exp\left(z\epsilon + \epsilon^2\right), \tag{2.23}$$

with $p_j(z) \equiv 0$ for $j < 0$. Then, generalized Okamoto polynomials $Q_{N_1,N_2}(z)$, with N_1, N_2 being nonnegative integers, are defined as

$$Q_{N_1,N_2}(z) = \mathrm{Wron}[p_2, p_5, \cdots, p_{3N_1-1}, p_1, p_4, \cdots, p_{3N_2-2}], \tag{2.24}$$

or equivalently,

$$Q_{N_1,N_2}(z) = \begin{vmatrix} p_2 & p_1 & \cdots & p_{3-N_1-N_2} \\ \vdots & \vdots & \vdots & \vdots \\ p_{3N_1-1} & p_{3N_1-2} & \cdots & p_{2N_1-N_2} \\ p_1 & p_0 & \cdots & p_{2-N_1-N_2} \\ \vdots & \vdots & \vdots & \vdots \\ p_{3N_2-2} & p_{3N_2-3} & \cdots & p_{2N_2-N_1-1} \end{vmatrix}, \tag{2.25}$$

since $p'_{j+1}(z) = p_j(z)$ from the definition of $p_j(z)$ in Eq. (2.23), where the prime represents differentiation. The first few $Q_{N_1,N_2}(z)$ polynomials are

$$Q_{1,0}(z) = \frac{1}{2}(z^2 + 2),$$
$$Q_{2,0}(z) = \frac{1}{80}(z^6 + 10z^4 + 20z^2 + 40),$$
$$Q_{0,1}(z) = z,$$
$$Q_{1,1}(z) = \frac{1}{2}(-z^2 + 2)$$
$$Q_{2,1}(z) = \frac{1}{20}z(z^4 - 20),$$
$$Q_{0,2}(z) = \frac{1}{8}(z^4 + 4z^2 - 4),$$
$$Q_{1,2}(z) = \frac{1}{8}(-z^4 + 4z^2 + 4),$$
$$Q_{2,2}(z) = \frac{1}{80}(-z^6 + 10z^4 - 20z^2 + 40).$$

Note that our definition of generalized Okamoto polynomials is different from that by Clarkson in Refs. [24,25]. Denoting the $Q_{m,n}(z)$ polynomial introduced in [24,25] as $Q^{[C]}_{m,n}(z)$, then our polynomial $Q_{N_1,N_2}(z)$ is related to $Q^{[C]}_{m,n}(z)$ as

$$Q_{N_1,N_2}(z) = \begin{cases} \gamma^{(1)}_{N_1,N_2} Q^{[C]}_{N_2-N_1,-N_2}\left(\sqrt{3}\,z/2\right), & N_1 \geq N_2, \\ \gamma^{(2)}_{N_1,N_2} Q^{[C]}_{N_2-N_1,N_1+1}\left(\sqrt{3}\,z/2\right), & N_1 \leq N_2, \end{cases} \tag{2.26}$$

where $\gamma^{(1)}_{N_1,N_2}$ and $\gamma^{(2)}_{N_1,N_2}$ are certain real constants.

Clarkson [24] observed an interesting symmetry relation between $Q^{[C]}_{n,m}(z)$ and $Q^{[C]}_{m,n}(\mathrm{i}z)$ based on examples (see Eq. (4.9) in that paper). Using that symmetry and the above polynomial connection (2.26), we obtain symmetry relations for our polynomials $Q_{N_1,N_2}(z)$ as

$$Q_{N_1,N_1-N_2}(z) = b_1 e^{-\frac{1}{2}\mathrm{i}\pi d_{N_1,N_2}} Q_{N_1,N_2}(\mathrm{i}z), \quad N_1 \geq N_2, \tag{2.27}$$
$$Q_{N_2-N_1-1,N_2}(z) = b_2 e^{-\frac{1}{2}\mathrm{i}\pi d_{N_1,N_2}} Q_{N_1,N_2}(\mathrm{i}z), \quad N_1 < N_2, \tag{2.28}$$

where

$$d_{N_1,N_2} = N_1^2 + N_2^2 - N_1N_2 + N_1 \tag{2.29}$$

is the degree of the $Q_{N_1,N_2}(z)$ polynomial, $b_1 = \pm 1$ is the sign of the ratio between coefficients of the highest z-power terms in $Q_{N_1,N_2}(z)$ and $Q_{N_1,N_1-N_2}(z)$, while $b_2 = \pm 1$ is the sign of the ratio between coefficients of the highest z-power terms in $Q_{N_1,N_2}(z)$

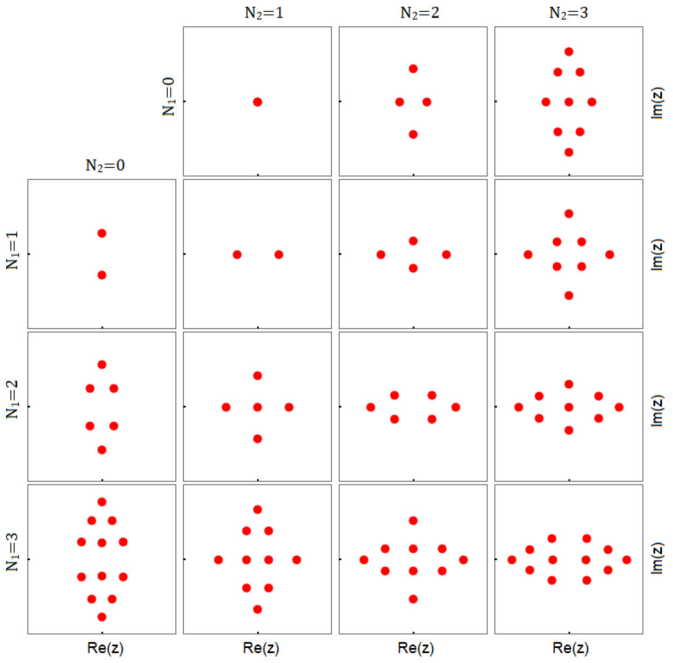

Fig. 2. Roots of generalized Okamoto polynomials $Q_{N_1,N_2}(z)$ in the complex z plane for $0 \le N_1, N_2 \le 3$. In all panels, $-5 \le \mathrm{Re}(z), \mathrm{Im}(z) \le 5$.

and $Q_{N_2-N_1-1,\,N_2}(z)$. In the special case of $N_2 = 0$, the symmetry (2.27) further reduces to

$$Q_{N_1,N_1}(z) = Q_{N_1,0}(\mathrm{i}z). \tag{2.30}$$

For our partial-rogue wave problem, it turns out from later text that we need generalized Okamoto polynomials which have either real or imaginary roots, but not both. In addition, zero cannot be a root. To identify such polynomials, we plot in Fig. 2 roots of $Q_{N_1,N_2}(z)$ in the complex z plane for $0 \le N_1, N_2 \le 3$. We can see from this figure that the polynomials that fit our requirements are $Q_{N_1,0}(z)$ and $Q_{N_1,N_1}(z)$ polynomials, which lie in the first column and on the diagonal of Fig. 2, respectively. The $Q_{N_1,0}(z)$ polynomials in the first column have only imaginary roots but not real roots. The $Q_{N_1,N_1}(z)$ polynomials on the diagonal have only real roots but not imaginary roots, which is not surprising given the connection between Q_{N_1,N_1} and $Q_{N_1,0}$ polynomials in Eq. (2.30). For both types of polynomials, zero is not a root. All other polynomials in Fig. 2 have both real and imaginary roots, and are thus not useful for the partial-rogue problem. We note by passing that these root structures in Fig. 2 are consistent with the two symmetries of generalized Okamoto polynomials in Eqs. (2.27)-(2.28).

Multiplicity of these nonzero real or imaginary roots is also important to us. Our numerical checking shows that nonzero roots are all simple for every generalized Okamoto polynomial. This will make our results of the next section a bit simpler.

3. Partial-rogue waves

According to our definition, partial-rogue waves are localized waves that "come from nowhere but leave with a trace". Thus, we impose the following boundary conditions

$$u(x,t) \to e^{\mathrm{i}[\alpha(x+6t)-\alpha^3 t]}, \quad t \to -\infty \text{ or } x \to \pm\infty, \tag{3.1}$$

where $\alpha = 1/2$. In addition, we require $u(x,t)$ not to approach this constant-amplitude background as $t \to +\infty$.

3.1. Two theorems on partial-rogue waves

Only a small portion of rational solutions in Theorem 1 are partial-rogue waves. This is not surprising, since the fundamental rational soliton in Fig. 1 is not a partial-rogue wave already. We will show that a rational solution in Theorem 1 is a partial-rogue wave only if the associated generalized Okamoto polynomial has either imaginary or real roots, but not both. This result is summarized in the following two theorems, for imaginary roots and real roots, respectively.

Theorem 2. *If the generalized Okamoto polynomial $Q_{N_1,N_2}(z)$ has imaginary but not real roots, and each imaginary root is simple, then the rational solution $u_{N_1,N_2}(x,t)$ in Theorem 1 with $p_0 = -\sqrt{3}/2$ is a partial-rogue wave. In addition, when $t \gg 1$, this solution splits into n fundamental rational solitons $\hat{u}_1(x - x_0^{(k)}, t)\, e^{\mathrm{i}[\frac{1}{2}(x+6t)-\frac{1}{8}t]}$, where n is the number of imaginary roots in $Q_{N_1,N_2}(z)$, and $1 \le k \le n$. The location $x_0^{(k)}$ of the k-th fundamental rational soliton is given by*

$$x_0^{(k)} = -\frac{33}{4}t - \mathrm{i}z_0^{(k)}\frac{3^{3/4}}{2^{1/2}}t^{1/2} + \frac{2}{12^{1/6}}\Delta^{(k)}, \tag{3.2}$$

where $z_0^{(k)}$ is the k-th imaginary root of $Q_{N_1,N_2}(z)$, and $\Delta^{(k)}$ is a $z_0^{(k)}$-dependent $O(1)$ quantity whose expression will be given by Eq. (4.22) in later text (upon replacing its z_0 with $z_0^{(k)}$ and Δ with $\Delta^{(k)}$). The error of this fundamental rational soliton approximation is $O(|t|^{-1/2})$. Expressed mathematically, if $t \gg 1$, and x is in an $O(1)$ neighborhood of $x_0^{(k)}$, i.e., $|x - x_0^{(k)}| = O(1)$, then

$$u_{N_1,N_2}(x,t) = \hat{u}_1(x - x_0^{(k)}, t)\, e^{\mathrm{i}[\frac{1}{2}(x+6t)-\frac{1}{8}t]} + O(|t|^{-1/2}). \tag{3.3}$$

When $t \to +\infty$ and x is not in an $O(1)$ neighborhood of any $x_0^{(k)}$, or when $t \to -\infty$ for all x, the solution approaches the constant-amplitude background (2.2), i.e.,

$$u_{N_1,N_2}(x,t) \to e^{\mathrm{i}[\frac{1}{2}(x+6t)-\frac{1}{8}t]}. \tag{3.4}$$

Theorem 3. *If the generalized Okamoto polynomial $Q_{N_1,N_2}(z)$ has real but not imaginary roots, and each real root is nonzero and simple, then the rational solution $u_{N_1,N_2}(x,t)$ in Theorem 1 with $p_0 = \sqrt{3}/2$ is a partial-rogue wave. In addition, when $t \gg 1$, this solution splits into n fundamental rational solitons $\hat{u}_1(x - x_0^{(k)}, t)\, e^{\mathrm{i}[\frac{1}{2}(x+6t)-\frac{1}{8}t]}$, where n is the number of real roots in $Q_{N_1,N_2}(z)$, and $1 \le k \le n$. The location $x_0^{(k)}$ of the k-th fundamental rational soliton is given by*

$$x_0^{(k)} = -\frac{33}{4}t + z_0^{(k)}\frac{3^{3/4}}{2^{1/2}}t^{1/2} - \frac{2}{12^{1/6}}\Delta^{(k)}, \tag{3.5}$$

where $z_0^{(k)}$ is the k-th real root of $Q_{N_1,N_2}(z)$, and $\Delta^{(k)}$ is a $z_0^{(k)}$-dependent $O(1)$ quantity whose expression will be given by Eq. (4.22) in later text (upon replacing its z_0 with $z_0^{(k)}$ and Δ with $\Delta^{(k)}$). The error of this fundamental rational soliton approximation is $O(|t|^{-1/2})$. Mathematical expressions of these results are the same as those in Eqs. (3.3)-(3.4) of Theorem 2, except for the different formula (3.5) for the soliton's location $x_0^{(k)}$.

Proofs of these two theorems will be given in the next section.

These two theorems, together with root structures of generalized Okamoto polynomials in Fig. 2, predict that rational solutions $u_{N_1,0}(x,t)$ $(N_1 \ge 1)$ with $p_0 = -\sqrt{3}/2$, as well as $u_{N_1,N_1}(x,t)$ $(N_1 \ge 1)$ with $p_0 = \sqrt{3}/2$, are partial-rogue waves. As $t \to -\infty$, they approach the constant-amplitude background. As $t \to +\infty$, they split into several fundamental rational solitons, and the number of such fundamental solitons is equal to the number of real

or imaginary roots in the underlying generalized Okamoto polynomial. These results are not dependent on values of internal parameters $a_{r,1}, a_{r,2}$ $(r = 1, 2, \cdots)$. This is not surprising, since when $|t| \gg 1$, those internal parameters in the solution will play a less significant role.

3.2. Analytical expressions for simplest partial-rogue waves

The simplest partial-rogue wave in the $u_{N_1,0}(x,t)$ family is $u_{1,0}(x,t)$ with $p_0 = -\sqrt{3}/2$, whose explicit expression is

$$u_{1,0}(x,t) = \frac{\sigma_{1,0}(\hat{x},t)}{\sigma_{0,0}(\hat{x},t)} e^{\mathrm{i}[\frac{1}{2}(x+6t)-\frac{1}{8}t]}, \tag{3.6}$$

where

$$\sigma_{k,0}(\hat{x},t) = \left(\frac{1}{2}\left[x_{1,1}^{+}(k)\right]^2 + x_{2,1}^{+}(k)\right)\left(\frac{1}{2}\left[x_{1,1}^{-}(k)\right]^2 + x_{2,1}^{-}(k)\right) + \left(\frac{p_1^2}{4p_0^2}\right) x_{1,1}^{+}(k) x_{1,1}^{-}(k) + \left(\frac{p_1^2}{4p_0^2}\right)^2,$$

$$x_{1,1}^{+}(k) = p_1\hat{x} + k\theta_1 + a_{1,1},$$

$$x_{1,1}^{-}(k) = p_1\hat{x} - k\theta_1^{*} + a_{1,1},$$

$$x_{2,1}^{+}(k) = p_2\hat{x} + (9p_2/2)t + k\theta_2 + a_{2,1},$$

$$x_{2,1}^{-}(k) = p_2\hat{x} + (9p_2/2)t - k\theta_2^{*} + a_{2,1},$$

$\hat{x}$ is as defined in Eq. (2.22), i.e., $\hat{x} = x + 33t/4$, (p_1, p_2) values are opposite of those in Eq. (2.16) and (θ_1, θ_2) values the complex conjugates of those in Eq. (2.18) since $p_0 = -\sqrt{3}/2$, and $(a_{1,1}, a_{2,1})$ are free real constants.

From the above solution expression, it is easy to see that through a shift of the $(\hat{x}, t)$ axes, we can normalize

$$a_{1,1} = a_{2,1} = 0 \tag{3.7}$$

without any loss of generality. For similar reasons, this zero normalization of $a_{1,1}$ and $a_{2,1}$ can be achieved for all partial-rogue waves $u_{N_1,0}(x,t)$ and $u_{N_1,N_1}(x,t)$.

Under this parameter normalization, expressions for $\sigma_{0,0}$ and $\sigma_{1,0}$ in Eq. (3.6) can be reduced to

$$\sigma_{0,0}(\hat{x},t) = 4 + 243t^2 + 24\hat{x}^2 - 12\sqrt{3}\hat{x}^3 + 9\hat{x}^4 + 54t\hat{x}\left(2 - \sqrt{3}\hat{x}\right), \tag{3.8}$$

$$\sigma_{1,0}(\hat{x},t) = -2 + 6\mathrm{i}\sqrt{3} + 243t^2 - 12\mathrm{i}\hat{x} - \left(3 + 9\mathrm{i}\sqrt{3}\right)\hat{x}^2 + 6\left(3\mathrm{i} - 2\sqrt{3}\right)\hat{x}^3 + 9\hat{x}^4 - 27t\left[\mathrm{i} + \sqrt{3} + 2\mathrm{i}\left(2\mathrm{i} + \sqrt{3}\right)\hat{x} + 2\sqrt{3}\hat{x}^2\right], \tag{3.9}$$

which do not contain any free parameters. The graph of this solution, in the $(\hat{x}, t)$ plane, will be plotted in Fig. 3(a) of the next subsection.

The simplest partial-rogue wave in the $u_{N_1,N_1}(x,t)$ family is $u_{1,1}(x,t)$ with $p_0 = \sqrt{3}/2$. Under parameter normalization (3.7), this $u_{1,1}(x,t)$ solution still contains a free real parameter $a_{1,2}$. However, we have found that this $u_{1,1}(x,t)$ solution can be simplified as

$$u_{1,1}(x,t) = \frac{\sigma_{1,0}(\tilde{x},\tilde{t})}{\sigma_{0,0}(\tilde{x},\tilde{t})} e^{\mathrm{i}[\frac{1}{2}(x+6t)-\frac{1}{8}t]}, \tag{3.10}$$

where functions $\sigma_{0,0}$ and $\sigma_{1,0}$ are as given in Eqs. (3.8)-(3.9), and

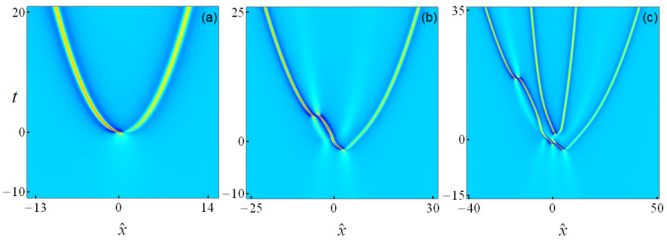

Fig. 3. Density plots of partial-rogue waves $|u_{1,0}(x,t)|$ (a), $|u_{2,0}(x,t)|$ (b), and $|u_{3,0}(x,t)|$ (c), with $p_0 = -\sqrt{3}/2$ and internal parameter values in Eqs. (3.13), (3.14), and (3.15), respectively. The horizontal axes are $\hat{x} = x + (33/4)t$.

$$\tilde{x} = \hat{x} + \frac{2^{2/3}}{3^{1/6}} a_{1,2}, \tag{3.11}$$

$$\tilde{t} = t - \frac{2^{5/3}}{3^{13/6}} a_{1,2} + \frac{2^{4/3}}{3^{11/6}} a_{1,2}^2. \tag{3.12}$$

Thus, under a shift of the $(\hat{x}, t)$ axes, the $u_{1,1}(x,t)$ solution with free parameter $a_{1,2}$ reduces to the $u_{1,0}(x,t)$ solution given in Eqs. (3.6) and (3.8)-(3.9). This $u_{1,1}(x,t)$ solution, in the $(\hat{x}, t)$ plane with $a_{1,2} = 3$, will be plotted in Fig. 5(a) of the next subsection.

Since the $u_{1,1}(x,t)$ solution is equivalent to the $u_{1,0}(x,t)$ solution, one may wonder if $u_{N_1,N_1}(x,t)$ solutions are equivalent to $u_{N_1,0}(x,t)$ solutions in general, i.e., for all $N_1 \geq 1$, even though $u_{N_1,N_1}(x,t)$ contains more free parameters than $u_{N_1,0}(x,t)$. This is an interesting question that merits further studies in the future.

3.3. Numerical verifications of the two theorems

Next, we numerically verify these two theorems. First, we consider Theorem 2. Based on Fig. 2, this theorem predicts that rational solutions $u_{1,0}$, $u_{2,0}$, and $u_{3,0}$, with $p_0 = -\sqrt{3}/2$, are partial-rogue waves. To verify this, we take internal parameters in these three solutions respectively as

$$a_{1,1} = a_{2,1} = 0, \tag{3.13}$$

$$a_{1,1} = a_{2,1} = 0,\ a_{4,1} = 2,\ a_{5,1} = -3, \tag{3.14}$$

$$a_{1,1} = a_{2,1} = 0,\ a_{4,1} = 2,\ a_{5,1} = -3,\ a_{7,1} = a_{8,1} = 0. \tag{3.15}$$

The corresponding true solutions are plotted from Theorem 1 and displayed in Fig. 3. As can be seen, these are indeed partial-rogue waves that arise from the constant background but do not retreat back to it, in agreement with Theorem 2.

Theorem 2 also predicts that, as $t \to +\infty$, these partial-rogue waves would split into several fundamental rational solitons. Fig. 3 confirms that this is indeed the case. The reader may notice that individual fundamental solitons at large time in Fig. 3 appear to have different heights, while Theorem 2 predicts these fundamental solitons should approach the same height. It turns out that this discrepancy is due to the fact that the time shown in Fig. 3 is not large enough. We have checked that as time increases further, all these humps indeed approach the same height 2, which is the height of the fundamental rational soliton (2.20). To demonstrate, we choose the $|u_{2,0}(x,t)|$ solution in Fig. 3(b), and track the heights of its two humps versus time. The corresponding graphs are plotted in the left panel of Fig. 4. The height 2 of the fundamental soliton is also shown for comparison. One can see that the heights of both humps monotonically approach the height of the fundamental soliton as $t \to +\infty$, in agreement with Theorem 2.

To show further quantitative comparison, we again choose the $|u_{2,0}(x,t)|$ solution in Fig. 3(b). This time, we track true locations of its two humps at each large time, and compare them to predicted locations (3.2) in Theorem 2. The errors of these predictions, defined as the absolute difference between true and predicted hump

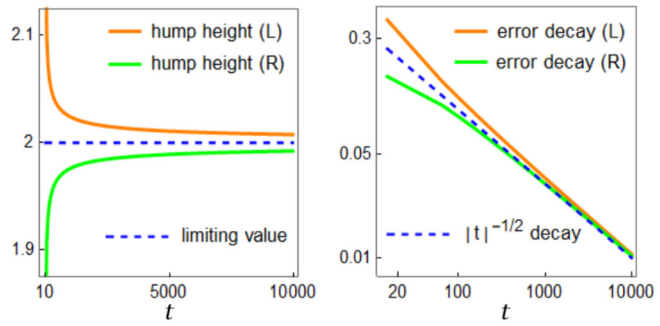

Fig. 4. Quantitative comparison between the true partial-rogue solution of Fig. 3(b) and its prediction from Theorem 2. Left: graphs of the two humps' heights versus time (upper one for the left hump and lower one for the right hump); the theoretical limiting value of 2 is also shown (as dashed line) for comparison. Right: errors versus time for predicted locations of the two humps at large time; the $|t|^{-1/2}$ decay is also plotted for comparison. (For interpretation of the colors in the figure(s), the reader is referred to the web version of this article.)

locations, versus time are plotted in the right panel of Fig. 4. This panel shows that the errors decay at the rate of $O(|t|^{-1/2})$, which matches our error estimate in the asymptotics (3.3). Thus, Theorem 2 is fully confirmed.

Now, we examine peak amplitudes of these partial-rogue waves in Fig. 3. The peak amplitude of $u_{1,0}(x,t)$ in Fig. 3(a) is found to be approximately 2.8371, which is reached at $(x,t)\approx(-0.2595, 0.0836)$. Recalling that the amplitude of our background has been normalized to unity [see (2.2)], this means that the $u_{1,0}(x,t)$ solution can reach a peak amplitude that is 2.8371 times the background amplitude. This 2.8371 value is similar to peak amplitudes of fundamental rogue waves in the Sasa-Satsuma equation as reported in [11–17,19].

For the other two partial-rogue waves $u_{2,0}(x,t)$ and $u_{3,0}(x,t)$ in Fig. 3(b, c), their peak amplitudes are approximately 2.8718 and 2.8519, respectively.

Next, we numerically confirm Theorem 3. Based on Fig. 2, this theorem predicts that rational solutions $u_{1,1}(x,t)$, $u_{2,2}(x,t)$, and $u_{3,3}(x,t)$ with $p_0=\sqrt{3}/2$ are partial-rogue waves. To verify this, we take internal parameters in these three solutions respectively as

$$a_{1,1}=a_{2,1}=0,\ a_{1,2}=3, \tag{3.16}$$

$$a_{1,1}=a_{2,1}=a_{4,1}=a_{5,1}=0,\ a_{1,2}=a_{2,2}=a_{4,2}=3, \tag{3.17}$$

$$a_{1,1}=a_{2,1}=a_{4,1}=a_{5,1}=a_{7,1}=a_{8,1}=0,$$

$$a_{1,2}=a_{2,2}=a_{4,2}=a_{5,2}=a_{7,2}=3. \tag{3.18}$$

The corresponding true solutions are plotted from Theorem 1 and displayed in Fig. 5. We can see that these are indeed partial-rogue waves, in agreement with Theorem 3. We have also done quantitative comparison between these true partial-rogue waves and their theoretical predictions in Theorem 3, similar to what we did in Fig. 4. That comparison also confirmed Theorem 3 quantitatively. Details will be omitted for brevity.

Regarding peak amplitudes of these partial-rogue waves in Fig. 5, their values are approximately 2.8371, 3.0165 and 3.2472, respectively.

4. Proofs of theorems

The proofs of Theorems 2 and 3 follow the asymptotic analysis we developed in [26–28] for rogue patterns in integrable systems and lump patterns in the Kadomtsev-Petviashvili I equation.

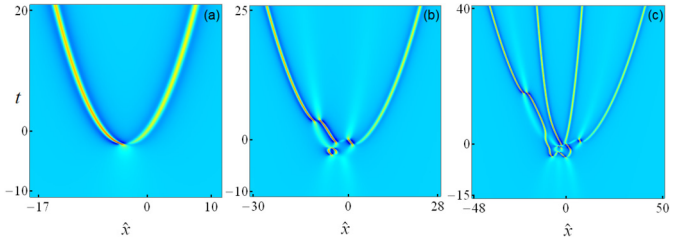

Fig. 5. Density plots of partial-rogue waves $|u_{1,1}(x,t)|$ (a), $|u_{2,2}(x,t)|$ (b), and $|u_{3,3}(x,t)|$ (c), with $p_0=\sqrt{3}/2$ and internal parameter values in Eqs. (3.16), (3.17), and (3.18), respectively. The horizontal axes are $\hat{x}=x+(33/4)t$.

Proof of Theorem 2. To prove Theorem 2, we first rewrite $\sigma_{k,l}$ in Eq. (2.6) as a larger determinant with simpler matrix elements [26, 29]

$$\sigma_{k,l}=\begin{vmatrix} \mathbf{O}_{N\times N} & \Phi_{N\times\widehat{N}} \\ -\Psi_{\widehat{N}\times N} & \mathbf{I}_{\widehat{N}\times\widehat{N}} \end{vmatrix}, \tag{4.1}$$

where $N=N_1+N_2$, $\widehat{N}=\max(3N_1,3N_2-1)$,

$$\Phi_{i,j}^{(k,l)}=\begin{cases} h_0^{j-1}S_{3i-j}\left(\boldsymbol{x}_1^+(k,l)+(j-1)\boldsymbol{s}\right), & i\le N_1,\\ h_0^{j-1}S_{3(i-N_1)-j-1}\left(\boldsymbol{x}_2^+(k,l)+(j-1)\boldsymbol{s}\right), & i>N_1,\end{cases}$$

$$\Psi_{i,j}^{(k,l)}=\begin{cases} h_0^{i-1}S_{3j-i}\left(\boldsymbol{x}_1^-(k,l)+(i-1)\boldsymbol{s}\right), & j\le N_1,\\ h_0^{i-1}S_{3(j-N_1)-i-1}\left(\boldsymbol{x}_2^-(k,l)+(i-1)\boldsymbol{s}\right), & j>N_1,\end{cases}$$

and $h_0\equiv p_1/2p_0$. Next, we apply the Laplace expansion to Eq. (4.1) and get

$$\sigma_{k,l}=\sum_{0\le\nu_1<\nu_2<\cdots<\nu_N\le\widehat{N}-1}\det_{1\le i,j\le N}\Phi_{i,\nu_j}^{(k,l)}\times\det_{1\le i,j\le N}\Psi_{i,\nu_j}^{(k,l)}. \tag{4.2}$$

To analyze $\sigma_{k,l}$'s large-time behavior, we need large-time asymptotics of $S_j(\boldsymbol{x}_l^{\pm}(k,l)+\nu\boldsymbol{s})$. Notice that for $|x|\gg1$ and $|t|\gg1$,

$$x_{1,l}^+(k,l)\sim p_1(x+6t)+\beta_1 t=p_1\hat{x}, \tag{4.3}$$

where $\hat{x}$ is as defined in (2.22), and $I=1,2$. Similarly,

$$x_{2,l}^+(k,l)\sim p_2\hat{x}+\mu_2 t,\quad x_{3,l}^+(k,l)\sim p_3\hat{x}+\mu_3 t, \tag{4.4}$$

where

$$\mu_2=9p_2/2,\quad \mu_3=12p_3. \tag{4.5}$$

Thus, when $|t|\gg1$ and $\hat{x}=O(|t|^{1/2})$, we have the following leading-order asymptotics

$$S_j\left(\boldsymbol{x}_l^+(k,l)+\nu\boldsymbol{s}\right)\sim S_j(\mathbf{v}), \tag{4.6}$$

where

$$\mathbf{v}=\left(p_1\hat{x},\ \mu_2 t,\ 0,\ 0,\cdots\right). \tag{4.7}$$

By comparing the definition of Schur polynomials $S_j(\mathbf{v})$ in (2.3) to the definition of $p_j(z)$ polynomials in (2.23), we see that

$$S_j(\mathbf{v})=(\mu_2 t)^{j/2}\,p_j(z), \tag{4.8}$$

where

$$z\equiv\frac{p_1\hat{x}}{\sqrt{\mu_2 t}}. \tag{4.9}$$

Using these results and similar ones for $S_j(\boldsymbol{x}_l^-(k,l)+\nu\boldsymbol{s})$, we find that the leading-order term of $\sigma_{k,l}$ in Eq. (4.2) is

$$\sigma_{k,l}\sim h_0^{2m_0}(\mu_2 t)^{n_0}\,Q_{N_1,N_2}^2(z),\quad |t|\gg1, \tag{4.10}$$

where m_0 and n_0 are certain positive integers. Since $p_0 < 0$ in Theorem 2, $\mu_2 < 0$. Thus, for large negative time, z in Eq. (4.9) is real. Then, Eq. (4.10) tells us that, if $Q_{N_1,N_2}(z)$ does not have real roots as assumed in Theorem 2, the above leading-order asymptotics for $\sigma_{k,l}$ would not vanish. Since this asymptotics is independent of (k,l), then $\sigma_{1,0}/\sigma_{0,0}$ would approach 1 when $t \to -\infty$, which means that

$$u_{N_1,N_2}(x,t) \to e^{\mathrm{i}[\frac{1}{2}(x+6t)-\frac{1}{8}t]}, \quad t \to -\infty, \tag{4.11}$$

in view of Eq. (2.4).

When $t \gg 1$, z in Eq. (4.9) is imaginary. If this z value is not near an imaginary root z_0 of the $Q_{N_1,N_2}(z)$ polynomial, i.e., $|\hat{x} - \hat{x}_0| \gg 1$, where

$$\hat{x}_0 = \frac{\sqrt{\mu_2 t}}{p_1} z_0 = -\mathrm{i} z_0 \frac{3^{3/4}}{2^{1/2}} t^{1/2}, \tag{4.12}$$

then the leading-order asymptotics (4.10) does not vanish either. For similar reasons as above, $u_{N_1,N_2}(x,t)$ would approach the background $e^{\mathrm{i}[\frac{1}{2}(x+6t)-\frac{1}{8}t]}$ as well.

When $t \gg 1$ and $|\hat{x} - \hat{x}_0| = O(1)$, the z value from Eq. (4.9) is near z_0, and the leading-order asymptotics (4.10) breaks down. In this case, a more refined asymptotic analysis is needed. The starting point is a more refined asymptotics for $S_j\left(\boldsymbol{x}_I^+(k,l) + \nu \boldsymbol{s}\right)$,

$$S_j\left(\boldsymbol{x}_I^+(k,l) + \nu \boldsymbol{s}\right) = S_j\left(\hat{\mathbf{v}}_I\right)\left(1 + O(|t|^{-1})\right), \tag{4.13}$$

where

$$\hat{\mathbf{v}}_I = \left(x_{1,I}^+(k,l),\, p_2\hat{x} + \mu_2 t,\, \mu_3 t,\, 0,\, 0,\, \cdots\right). \tag{4.14}$$

Here, the fact of $s_1 = 0$ has been utilized. Let us split $\hat{\mathbf{v}}_1$ and $\hat{\mathbf{v}}_2$ as

$$\hat{\mathbf{v}}_1 = \mathbf{w} + \left(0,\, p_2\hat{x},\, \mu_3 t,\, 0,\, 0,\, \cdots\right), \tag{4.15}$$

$$\hat{\mathbf{v}}_2 = \mathbf{w} + \left(a_{1,2} - a_{1,1},\, p_2\hat{x},\, \mu_3 t,\, 0,\, 0,\, \cdots\right), \tag{4.16}$$

where

$$\mathbf{w} \equiv \left(x_{1,1}^+(k,l),\, \mu_2 t,\, 0,\, 0,\, \cdots\right). \tag{4.17}$$

Then, using the definition (2.3) of Schur polynomials, we can readily find that

$$\begin{aligned} S_j\left(\boldsymbol{x}_1^+(k,l) + \nu \boldsymbol{s}\right) &= \left[S_j(\mathbf{w}) + p_2\hat{x}_0\, S_{j-2}(\mathbf{w}) + \mu_3 t\, S_{j-3}(\mathbf{w})\right] \\ &\quad \times \left(1 + O(|t|^{-1})\right), \end{aligned} \tag{4.18}$$

$$\begin{aligned} S_j\left(\boldsymbol{x}_2^+(k,l) + \nu \boldsymbol{s}\right) &= \left[S_j(\mathbf{w}) + (a_{1,2} - a_{1,1}) S_{j-1}(\mathbf{w}) \right. \\ &\quad \left. + p_2\hat{x}_0\, S_{j-2}(\mathbf{w}) + \mu_3 t\, S_{j-3}(\mathbf{w})\right] \\ &\quad \times \left(1 + O(|t|^{-1})\right), \end{aligned} \tag{4.19}$$

where

$$\begin{aligned} S_j(\mathbf{w}) &= (\mu_2 t)^{j/2}\, p_j\left(\frac{x_{1,1}^+(k,l)}{\sqrt{\mu_2 t}}\right) \\ &= (\mu_2 t)^{j/2}\, p_j\left(z_0 + \frac{p_1(\hat{x} - \hat{x}_0) + k\theta_1 + l\theta_1^* + a_{1,1}}{\sqrt{\mu_2 t}}\right). \end{aligned} \tag{4.20}$$

Similar asymptotics can be obtained for $S_j\left(\boldsymbol{x}_I^-(k,l) + \nu \boldsymbol{s}\right)$.

Now, we use these refined asymptotics of $S_j\left(\boldsymbol{x}_I^{\pm}(k,l) + \nu \boldsymbol{s}\right)$ to determine the leading-order asymptotics of $\sigma_{k,l}$ from Eq. (4.2). This leading-order asymptotics comes from two index-vector contributions, one being $\nu = (0,1,2,\cdots,N-2,N-1)$, and the other being $\nu = (0,1,2,\cdots,N-2,N)$. For the first index vector, there are two sources of contributions to $\det_{1\le i,j\le N} \Phi_{i,\nu_j}^{(k,l)}$. One is when the $S_j(\mathbf{w})$ term in (4.18)-(4.19) is chosen in each $\Phi_{i,\nu_j}^{(k,l)}$ element. In view of Eq. (4.20), this part of the contribution amounts to

$$h_0^{m_0}(\mu_2 t)^{(n_0-1)/2}\left(p_1(\hat{x} - \hat{x}_0) + k\theta_1 + l\theta_1^* + a_{1,1}\right) Q'_{N_1,N_2}(z_0),$$

where m_0 and n_0 are the same as those in Eq. (4.10). The other source of contributions to $\det_{1\le i,j\le N} \Phi_{i,\nu_j}^{(k,l)}$ comes from taking the $S_j(\mathbf{w})$ term of (4.18)-(4.19) in all columns of the $\Phi_{i,\nu_j}^{(k,l)}$ matrix, except for a single column where the $S_{j-1}(\mathbf{w})$, $S_{j-2}(\mathbf{w})$, and $S_{j-3}(\mathbf{w})$ terms of (4.18)-(4.19) are chosen. Recalling the $\hat{x}_0$ formula (4.12), this part of the contribution amounts to

$$\begin{aligned} h_0^{m_0}(\mu_2 t)^{(n_0-1)/2} \sum_{j=1}^{N} \Bigg[& (a_{1,2} - a_{1,1}) Q_j^{(1)}(z_0) + \frac{p_2}{p_1} z_0 Q_j^{(2)}(z_0) \\ & + \frac{\mu_3}{\mu_2} Q_j^{(3)}(z_0)\Bigg], \end{aligned}$$

where $Q_j^{(1)}(z)$ is the $Q_{N_1,N_2}(z)$ determinant (2.25), but with its j-th column modified so that its first N_1 elements become zero, and its remaining elements are the original $p_n(z)$'s with their indices n reduced by one each, and $Q_j^{(2)}(z)$, $Q_j^{(3)}(z)$ are the $Q_{N_1,N_2}(z)$ determinants (2.25) but with $p_n(z)$ indices n of their j-th column reduced by two and three, respectively. Contributions to $\det_{1\le i,j\le N} \Psi_{i,\nu_j}^{(k,l)}$ of (4.2) can be obtained similarly.

For the second index vector of $\nu = (0,1,2,\cdots,N-2,N)$ in Eq. (4.2), leading-order contributions to $\det_{1\le i,j\le N} \Phi_{i,\nu_j}^{(k,l)}$ only come from choosing the $S_j(\mathbf{w})$ term of (4.18)-(4.19) in each $\Phi_{i,\nu_j}^{(k,l)}$ element, and this contribution amounts to

$$h_0^{m_0-1}(\mu_2 t)^{(n_0-1)/2} Q'_{N_1,N_2}(z_0)$$

in view of the relation $p'_{j+1}(z) = p_j(z)$. A similar result can be obtained for $\det_{1\le i,j\le N} \Psi_{i,\nu_j}^{(k,l)}$.

Collecting these results, we find that the leading-order contribution to $\sigma_{k,l}$ in Eq. (4.2) is

$$\begin{aligned} \sigma_{k,l} \sim h_0^{2m_0}(\mu_2 t)^{n_0-1} Q'^2_{N_1,N_2}(z_0) \Big[& \left(p_1(\hat{x} - \hat{x}_0) + k\theta_1 + l\theta_1^* + \Delta\right) \\ & \times \left(p_1(\hat{x} - \hat{x}_0) - k\theta_1^* - l\theta_1 + \Delta\right) + h_0^{-2}\Big], \end{aligned} \tag{4.21}$$

where

$$\Delta = a_{1,1} + \frac{\sum_{j=1}^{N}\left[\hat{a}_1 Q_j^{(1)}(z_0) + \frac{p_2}{p_1} z_0 Q_j^{(2)}(z_0) + \frac{\mu_3}{\mu_2} Q_j^{(3)}(z_0)\right]}{Q'_{N_1,N_2}(z_0)}, \tag{4.22}$$

and $\hat{a}_1 \equiv a_{1,2} - a_{1,1}$. If $N_2 = 0$, where the parameter $a_{1,2}$ does not arise in the $u_{N_1,N_2}(x,t)$ solution (2.4), then the $\hat{a}_1 Q_j^{(1)}(z_0)$ term in the above Δ formula would disappear. Since the imaginary root z_0 of $Q_{N_1,N_2}(z)$ is simple according to our assumption, $Q'_{N_1,N_2}(z_0) \neq 0$. Thus, the above leading-order asymptotics of $\sigma_{k,l}$ does not vanish. This asymptotics, when inserted into Eq. (2.4), gives a fundamental rational soliton $\hat{u}_1(x - x_0, t) e^{\mathrm{i}[\frac{1}{2}(x+6t)-\frac{1}{8}t]}$, where the soliton position x_0 can be obtained from $\hat{x}_0$ and Δ as

$$x_0 = -\frac{33}{4} t + \hat{x}_0 - \frac{\Delta}{p_1}, \tag{4.23}$$

which is the same as Eq. (3.2) in Theorem 2 since $p_1 = -12^{1/6}/2$ here. The relative error of the leading-order asymptotics (4.21) of $\sigma_{k,l}$ is $O(|t|^{-1/2})$, which leads to an error of $O(|t|^{-1/2})$ in the above fundamental-soliton approximation. This completes the proof of Theorem 2. □

Proof of Theorem 3. The proof of Theorem 3 is very similar to that of Theorem 2, and only very minor changes are needed. In this case, $p_0 > 0$ and $\mu_2 > 0$. Thus, for large negative time, z in Eq. (4.9) is imaginary. Then, if $Q_{N_1,N_2}(z)$ does not have imaginary roots as assumed in Theorem 3, the leading-order asymptotics (4.10) for $\sigma_{k,l}$ would not vanish. Hence, the asymptotics (4.11) holds, i.e., the solution $u_{N_1,N_2}(x,t)$ approaches the uniform background (2.2) when $t \to -\infty$.

When $t \gg 1$, z in Eq. (4.9) is real. If this z value is near a real root z_0 of $Q_{N_1,N_2}(z)$, i.e., $|\hat{x} - \hat{x}_0| = O(1)$, where

$$\hat{x}_0 = \frac{\sqrt{\mu_2 t}}{p_1} z_0 = z_0 \frac{3^{3/4}}{2^{1/2}} t^{1/2}, \tag{4.24}$$

then the leading-order asymptotics (4.10) breaks down, and a more refined asymptotics is needed. This more refined asymptotics is almost identical to that we developed in the proof of Theorem 2, starting from Eq. (4.13), because that refined asymptotics does not depend on the sign of p_0. In particular, Eq. (4.23) still holds here, except that the $\hat{x}_0$ formula should be updated to (4.24) now. Since $p_1 = 12^{1/6}/2$ here, we then get Eq. (3.5) in Theorem 3. The rest of Theorem 3 can be similarly obtained. Thus, Theorem 3 is proved. □

5. Other types of rational solutions

Rational solutions in Theorem 1 also contain other types of solutions. One other type is "waves that come from somewhere but leave without a trace" — the opposite of partial-rogue waves we considered earlier in this paper. Such solutions obviously exist, because the Sasa-Satsuma equation is invariant under the $(x,t) \to (-x,-t)$ transformation. Thus, from every partial-rogue wave, we can get such a new wave. This way of getting such new solutions will change the background condition (2.2) though. If we want to preserve that background, then we can just switch the sign of p_0 in Theorems 2 and 3, and the resulting solution would be "waves that come from somewhere but leave without a trace" instead of partial-rogue waves. As an example, we show in Fig. 6(a) such a solution by switching the sign of p_0 in the partial-rogue wave of Fig. 3(b). It is noted that a simpler solution of this type has been reported earlier in [14] (see Fig. 7(b) there). This type of solutions, although different, are closely related to partial-rogue waves. Thus, it is reasonable for us to call them partial-rogue waves as well for simplicity.

These partial-rogue waves are obtained when the associated generalized Okamoto polynomials have real but not imaginary roots, or imaginary but not real roots. As one can see from Fig. 2, most generalized Okamoto polynomials are not like that. For such polynomials, the associated rational solutions in Theorem 1 would not be partial-rogue waves. Instead, they would be solutions which split into several fundamental (or lower-order) rational solitons as time approaches both $\pm\infty$. As an example, we choose $(N_1, N_2) = (3,1)$ and $p_0 = \sqrt{3}/2$. The corresponding $Q_{3,1}(z)$ polynomial has four nonzero real roots and two imaginary roots, all of which are simple, see Fig. 2. Thus, a simple extension of our earlier asymptotic analysis predicts that, as t approaches $-\infty$, this solution would split into two fundamental rational solitons, but as t approaches $+\infty$, it would split into four fundamental rational solitons. To illustrate, we choose all internal parameters $a_{r,1}, a_{r,2}$ as zero. The resulting true solution from Theorem 1 is displayed in Fig. 6(b). This solution shows that, out of the interaction and collision of two fundamental rational solitons, four fundamental rational solitons emerge, in agreement with our predictions. This phenomenon is unusual and fascinating.

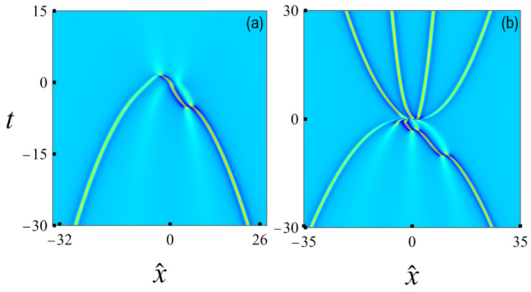

Fig. 6. Other types of rational solutions in Theorem 1. (a) A wave that comes from somewhere but leaves without a trace. This solution is obtained from $|u_{2,0}(x,t)|$ of Fig. 3(b), but with its p_0 value flipped from $-\sqrt{3}/2$ to $\sqrt{3}/2$. (b) A wave that comes and leaves with traces. This is the $|u_{3,1}(x,t)|$ solution with $p_0 = \sqrt{3}/2$ and all internal parameters as zero. In both panels, the horizontal axes are $\hat{x} = x + (33/4)t$.

6. Summary

In this article, we have asymptotically and numerically studied partial-rogue waves in the Sasa-Satsuma equation. We have shown that, among a class of rational solutions in this equation that can be expressed through determinants of 3-reduced Schur polynomials, partial-rogue waves would appear if these rational solutions are of certain orders, whose associated generalized Okamoto polynomials have real but not imaginary roots, or imaginary but not real roots. We have further shown that, these partial-rogue waves asymptotically approach the constant-amplitude background as time goes to negative infinity, but split into several fundamental rational solitons as time goes to positive infinity. Our asymptotic predictions are compared to true solutions both qualitatively and quantitatively, and excellent agreement has been obtained.

In earlier work [26–28], we linked rogue and lump patterns in the space-time plane to root structures of certain special polynomials in the complex plane. In that work, all roots of the special polynomials contributed to the space-time patterns of solutions. A distinctive feature of our present work is that, the question of partial-rogue waves and their large-time behaviors is linked to only real and imaginary roots of the underlying special polynomials (i.e., generalized Okamoto polynomials). Other complex roots of these polynomials are irrelevant. This feature vaguely resembles an earlier work in [30], where superluminal kinks in the semiclassical sine-Gordon equation were linked to real roots of Yablonskii-Vorob'ev polynomials. This wide variety of connections between nonlinear wave dynamics and certain types of roots in special polynomials is a remarkable phenomenon, and it reflects the richness of wave behaviors in nonlinear partial differential equations.

From a broader perspective, some other solutions are also related to partial-rogue waves. For example, in a two-dimensional multi-component long-wave-short-wave interaction system [31], some solutions describing a resonant collision between lumps and homoclinic orbits are such that the underlying lumps do not exist at large negative time but arise and persist at large positive time. But such solutions may not be called partial-rogue waves since they are not localized in space at intermediate times due to the nonlocal homoclinic-orbit component.

CRediT authorship contribution statement

Bo Yang: Writing – review & editing, Methodology, Investigation, Funding acquisition, Conceptualization. **Jianke Yang:** Writing – review & editing, Writing – original draft, Project administration, Methodology, Investigation, Funding acquisition, Conceptualization.

Declaration of competing interest

The authors declare that they have no known competing financial interests or personal relationships that could have appeared to influence the work reported in this paper.

Data availability

No data was used for the research described in the article.

Acknowledgement

The work of B.Y. was supported in part by the National Natural Science Foundation of China (Grant No.12201326), and the work of J.Y. was supported in part by the National Science Foundation (U.S.) under award number DMS-1910282.

Appendix A

In this appendix, we briefly derive rational solutions given in Theorem 1.

It has been shown in [17] that the Sasa-Satsuma equation (2.1) under boundary conditions (2.2) admits the following solutions

$$u(x,t) = e^{\mathrm{i}[\alpha(x+6t)-\alpha^3 t]}\ \frac{\tau_{1,0}}{\tau_{0,0}}\bigg|_{y=r=s=0}, \tag{A.1}$$

where

$$\tau_{k,l} = \det\begin{pmatrix} \tau_{k,l}^{[1,1]} & \tau_{k,l}^{[1,2]} \\ \tau_{k,l}^{[2,1]} & \tau_{k,l}^{[2,2]} \end{pmatrix}, \tag{A.2}$$

$$\tau_{k,l}^{[I,J]} = \left(\phi_{i_\nu^{[I]},\, j_\mu^{[J]}}^{(k,l\,I,\,J)}\right)_{1\le\nu\le N_I,\ 1\le\mu\le N_J}, \tag{A.3}$$

N_1 and N_2 are arbitrary non-negative integers, $\left(i_1^{[I]}, i_2^{[I]}, \cdots, i_{N_I}^{[I]}\right)$ and $\left(j_1^{[J]}, j_2^{[J]}, \cdots, j_{N_J}^{[J]}\right)$ are arbitrary sequences of non-negative indices,

$$\phi_{i,j}^{(k,l,I,J)} = \mathcal{A}_i\mathcal{B}_j\phi^{(k,l,I,J)}\Big|_{p=q,\ \xi_{0,I}(p)=\eta_{0,I}(q),\ \xi_{0,J}(p)=\eta_{0,J}(q)}, \tag{A.4}$$

$$\phi^{(k,l,I,J)} = \frac{1}{p+q}\left(-\frac{p-\mathrm{i}\alpha}{q+\mathrm{i}\alpha}\right)^k\left(-\frac{p+\mathrm{i}\alpha}{q-\mathrm{i}\alpha}\right)^l e^{\xi_I(p)+\eta_J(q)}, \tag{A.5}$$

$$\xi_I(p) = px + p^2y + p^3t + \frac{1}{p-\mathrm{i}\alpha}r + \frac{1}{p+\mathrm{i}\alpha}s + \xi_{0,I}(p), \tag{A.6}$$

$$\eta_J(q) = qx - q^2y + q^3t + \frac{1}{q+\mathrm{i}\alpha}r + \frac{1}{q-\mathrm{i}\alpha}s + \eta_{0,J}(q), \tag{A.7}$$

p is an arbitrary real number, $\xi_{0,1}(p)$ and $\xi_{0,2}(p)$ are arbitrary real functions of p, $\mathcal{A}_i$ and $\mathcal{B}_j$ are differential operators

$$\mathcal{A}_i = \frac{1}{i!}\left[f_1(p)\partial_p\right]^i, \quad \mathcal{B}_j = \frac{1}{j!}\left[f_2(q)\partial_q\right]^j, \tag{A.8}$$

and $f_1(p)$, $f_2(q)$ are arbitrary real functions, if the above $\tau_{k,l}$ satisfies the dimension reduction condition

$$(\partial_r + \partial_s + \partial_x)\,\tau_{k,l} = C\,\tau_{k,l}, \tag{A.9}$$

where C is some constant. The above result can be made even more general by allowing each of p and q to take different values in different blocks of the determinant (A.2) [17,20]. But that generalization is not necessary for our purpose.

Different ways to satisfy the dimension reduction condition (A.9) will lead to different types of solutions to the Sasa-Satsuma equation. One type of such solutions — rogue waves, were derived in [17]. To derive rational solutions in Theorem 1, a different dimension reduction is needed. Following the $\mathcal{W}$-p treatment we developed in [20,32], we first introduce the function $Q_1(p)$ as given in Eq. (2.13), i.e.,

$$Q_1(p) = \frac{1}{p-\mathrm{i}\alpha} + \frac{1}{p+\mathrm{i}\alpha} + p, \tag{A.10}$$

which is the coefficient of the exponential $(\partial_r + \partial_s + \partial_x)\,e^{\xi(p)}$. When $\alpha = 1/2$ as in Theorem 1, the equation $Q_1'(p) = 0$ has a pair of double real roots $p_0 = \pm\sqrt{3}/2$. In this case, we can show from [20] that the dimension reduction condition (A.9) would be satisfied if we choose

$$\tau_{k,l}^{[I,J]} = \left(\phi_{3i-I,\,3j-J}^{(k,l\,I,\,J)}\right)_{1\le i\le N_I,\ 1\le j\le N_J,\ p=p_0}, \tag{A.11}$$

$$f_1(p) = \frac{\mathcal{W}_1(p)}{\mathcal{W}_1'(p)}, \tag{A.12}$$

the function $\mathcal{W}_1(p)$ is determined from the equation

$$Q_1(p) = \frac{Q_1(p_0)}{3}\left(\mathcal{W}_1(p) + \frac{2}{\sqrt{\mathcal{W}_1(p)}}\cos\left[\frac{\sqrt{3}}{2}\ln\mathcal{W}_1(p)\right]\right), \tag{A.13}$$

and $f_2(q) = f_1(q)$. To introduce free parameters into these solutions, we choose $\xi_{0,I}(p)$ as

$$\xi_{0,I} = \sum_{r=1}^{\infty}\hat{a}_{r,I}\ln^r\mathcal{W}_1(p), \quad I = 1,2, \tag{A.14}$$

where $\hat{a}_{r,I}$ are free real constants.

Lastly, we simplify the matrix-element expression in Eq. (A.4) and derive a more explicit expression without differential operators in it. This can be done by following the technique developed in [20,29]. Repeating such calculations, we then derive the solution formulae in Theorem 1, where free real parameters $a_{r,I}$ are related to $\hat{a}_{r,I}$ of (A.14) as

$$a_{r,I} \equiv \hat{a}_{r,I} - b_r, \tag{A.15}$$

b_r is the real expansion coefficient of the function

$$\ln\left[\frac{p(\kappa)+p_0}{2p_0}\right] = \sum_{r=1}^{\infty}b_r\kappa^r, \tag{A.16}$$

and the real function $p(\kappa)$ is as defined in Eq. (2.12). It is noted that Eq. (2.12) admits three branches of $p(\kappa)$ functions, which are related to each other as $p(\kappa e^{\mathrm{i}2j\pi/3})$, where $j = 0, 1, 2$ (see Remark 3 in Ref. [20]). However, since $p(\kappa)$ in the current problem must be a real function, i.e., its Taylor expansion $p(\kappa) = \sum_{r=0}^{\infty}p_r\kappa^r$ must have real coefficients p_r, only one of those three branches is allowed.

References

[1] N. Akhmediev, A. Ankiewicz, M. Taki, Waves that appear from nowhere and disappear without a trace, Phys. Lett. A 373 (2009) 675–678.
[2] D.H. Peregrine, Water waves, nonlinear Schrödinger equations and their solutions, J. Aust. Math. Soc. B 25 (1983) 16.
[3] N. Akhmediev, A. Ankiewicz, J.M. Soto-Crespo, Rogue waves and rational solutions of the nonlinear Schrödinger equation, Phys. Rev. E 80 (2009) 026601.
[4] P. Dubard, P. Gaillard, C. Klein, V.B. Matveev, On multi-rogue wave solutions of the NLS equation and positon solutions of the KdV equation, Eur. Phys. J. Spec. Top. 185 (2010) 247.
[5] B. Kibler, J. Fatome, C. Finot, G. Millot, F. Dias, G. Genty, N. Akhmediev, J.M. Dudley, The Peregrine soliton in nonlinear fibre optics, Nat. Phys. 6 (2010) 790.
[6] A. Chabchoub, N. Hoffmann, N. Akhmediev, Rogue wave observation in a water wave tank, Phys. Rev. Lett. 106 (2011) 204502.

[7] Y. Ohta, J. Yang, Dynamics of rogue waves in the Davey-Stewartson II equation?, J. Phys. A 46 (2013) 105202.
[8] L.C. Zhao, S.C. Li, L. Ling, W-shaped solitons generated from a weak modulation in the Sasa-Satsuma equation, Phys. Rev. E 93 (2016) 032215.
[9] N. Sasa, J. Satsuma, New type of soliton solutions for a higher-order nonlinear Schrödinger equation, J. Phys. Soc. Jpn. 60 (1991) 409–417.
[10] Y. Kodama, A. Hasegawa, Nonlinear pulse propagation in a monomode dielectric guide, IEEE J. Quantum Electron. 23 (1987) 510–524.
[11] U. Bandelow, N. Akhmediev, Sasa-Satsuma equation: soliton on a background and its limiting cases, Phys. Rev. E 86 (2012) 026606.
[12] S. Chen, Twisted rogue-wave pairs in the Sasa-Satsuma equation, Phys. Rev. E 88 (2013) 023202.
[13] G. Mu, Z. Qin, Dynamic patterns of high-order rogue waves for Sasa-Satsuma equation, Nonlinear Anal., Real World Appl. 31 (2016) 179–209.
[14] L.M. Ling, The algebraic representation for high order solution of Sasa-Satsuma equation, Discrete Contin. Dyn. Syst., Ser. S 9 (2016) 1975–2010.
[15] G. Mu, Z. Qin, R. Grimshaw, N. Akhmediev, Intricate dynamics of rogue waves governed by the Sasa-Satsuma equation, Physica D 402 (2020) 132252.
[16] B.F. Feng, C. Shi, G. Zhang, C. Wu, Higher-order rogue wave solutions of the Sasa-Satsuma equation, J. Phys. A 55 (2022) 235701.
[17] C. Wu, G. Zhang, C. Shi, B.F. Feng, General rogue wave solutions to the Sasa-Satsuma equation, arXiv:2206.02210 [nlin.SI], 2022.
[18] L.C. Zhao, S.C. Li, L.M. Ling, Rational W-shaped solitons on a continuous-wave background in the Sasa-Satsuma equation, Phys. Rev. E 89 (2014) 023210.
[19] L. Guo, Y. Cheng, D. Mihalache, J.S. He, Darboux transformation and higher-order solutions of the Sasa-Satsuma equation, Rom. J. Phys. 64 (2019) 104.
[20] B. Yang, J. Yang, General rogue waves in the three-wave resonant interaction systems, IMA J. Appl. Math. 86 (2021) 378–425.
[21] K. Okamoto, Studies on the Painlevé equations III. Second and fourth Painlevé equations P_{II} and P_{IV}, Math. Ann. 275 (1986) 221–255.
[22] K. Kajiwara, Y. Ohta, Determinant structure of the rational solutions for the Painlevé IV equation, J. Phys. A 31 (1998) 2431–2446.
[23] M. Noumi, Y. Yamada, Symmetries in the fourth Painlevé equation and Okamoto polynomials, Nagoya Math. J. 153 (1999) 53–86.
[24] P.A. Clarkson, The fourth Painlevé equation and associated special polynomials, J. Math. Phys. 44 (2003) 5350–5374.
[25] P.A. Clarkson, Special polynomials associated with rational solutions of the defocusing nonlinear Schrödinger equation and the fourth Painlevé equation, Eur. J. Appl. Math. 17 (2006) 293–322.
[26] B. Yang, J. Yang, Rogue wave patterns in the nonlinear Schrodinger equation, Physica D 419 (2021) 132850.
[27] B. Yang, J. Yang, Universal rogue wave patterns associated with the Yablonskii-Vorob'ev polynomial hierarchy, Physica D 425 (2021) 132958.
[28] B. Yang, J. Yang, Pattern transformation in higher-order lumps of the Kadomtsev-Petviashvili I equation, J. Nonlinear Sci. 32 (2022) 52.
[29] Y. Ohta, J. Yang, General high-order rogue waves and their dynamics in the nonlinear Schrödinger equation, Proc. R. Soc. A 468 (2012) 1716–1740.
[30] R. Buckingham, P.D. Miller, The sine-Gordon equation in the semiclassical limit: critical behavior near a separatrix, J. Anal. Math. 118 (2012) 397–492.
[31] J. Rao, T. Kanna, D. Mihalache, J.S. He, Resonant collision of lumps with homoclinic orbits in the two-dimensional multi-component long-wave-short-wave resonance interaction systems, Physica D 439 (2022) 133281.
[32] B. Yang, J. Yang, General rogue waves in the Boussinesq equation, J. Phys. Soc. Jpn. 89 (2020) 024003.